

Cooper-pair splitting in two parallel InAs nanowires

S. Baba,^{1, a)} C. Jünger,^{2, b)} S. Matsuo,^{1, c)} A. Baumgartner,² Y. Sato,¹ H. Kamata,¹
K. Li,³ S. Jeppesen,⁴ L. Samuelson,⁴ H.-Q. Xu,^{3, 4} C. Schönenberger,^{2, d)} and S.
Tarucha^{1, 5, e)}

¹⁾*Department of Applied Physics, University of Tokyo, 7-3-1 Hongo, Bunkyo-ku, Tokyo 113-8656, Japan*

²⁾*Department of Physics, University of Basel, Klingelbergstrasse 82, CH-4056 Basel, Switzerland*

³⁾*Beijing Key Laboratory of Quantum Devices, Key Laboratory for the Physics and Chemistry of Nanodevices and Department of Electronics, Peking University, Beijing 100871, China*

⁴⁾*Division of Solid State Physics, Lund University, Box 118, SE-221 00 Lund, Sweden*

⁵⁾*Center for Emergent Matter Science, RIKEN, 2-1 Hirosawa, Wako-shi, Saitama 351-0198, Japan*

We report on the fabrication and electrical characterization of an InAs double - nanowire (NW) device consisting of two closely placed parallel NWs coupled to a common superconducting electrode on one side and individual normal metal leads on the other. In this new type of device we detect Cooper-pair splitting (CPS) with a sizeable efficiency of correlated currents in both NWs. In contrast to earlier experiments, where CPS was realized in a single NW, demonstrating an intrawire electron pairing mediated by the superconductor (SC), our experiment demonstrates an *inter-wire* interaction mediated by the common SC. The latter is the key for the realization of zero-magnetic field Majorana bound states, or Parafermions; in NWs and therefore constitutes a milestone towards topological superconductivity. In addition, we observe transport resonances that occur only in the superconducting state, which we tentatively attribute to Andreev Bound states and/or Yu-Shiba resonances that form in the proximitized section of one NW.

^{a)}These two authors contributed equally

^{b)}These two authors contributed equally; Electronic mail: christian.juenger@unibas.ch

^{c)}Electronic mail: matsuo@ap.t.u-tokyo.ac.jp

^{d)}Electronic mail: christian.schoenenberger@unibas.ch

^{e)}Electronic mail: tarucha@ap.t.u-tokyo.ac.jp

I. INTRODUCTION

Topologically protected electronic states in nanostructures have recently attracted wide attention, as they may provide fundamental building blocks for quantum computation.^{1,2} Recent advances in material science and device fabrication resulted in considerable progress towards the generation and detection of topologically protected bound states in topologically non-trivial semiconducting nanowires (NWs), so called Majorana Fermions (MF).³⁻⁷ Two MFs can combine together into a regular Fermion that is why MFs are also known as Z_2 Fermions. MFs are predicted to have non-Abelian braid statistics and may provide a platform for topological quantum computation.^{8,9} However, one can not implement all required operations for universal quantum computation in quantum bits (qubits) based on MFs by using topologically protected braiding. In this respect, Z_4 Fermions, also known as Parafermions (PFs), are better as they allow for a larger set of operations.¹⁰ Recently, it has theoretically been predicted that PFs can be generated in a system based on two NWs with different spin orbit interaction coupled to a common superconducting electrode.¹¹⁻¹³ The SC induces both a pairing interaction within each NW and between the two NWs due to Cooper-pair splitting (CPS). In order to realize PFs, the interwire coupling must dominate.¹² It has been shown that this is possible in systems with strong electron-electron interaction, such as nanoscaled semiconducting wires.¹⁴⁻¹⁶ Another advantage of the parallel two-wire approach, even if PFs are not formed, is the fact, that for large interwire pairing an external magnetic field is not required or only a small field is enough to reach the topological phase.¹⁷ A large magnetic field is a limiting factor, because of the critical magnetic field of the SC. It is therefore crucial both for MF-based charge qubits and for the realization of PFs to demonstrate an appreciable magnitude of interwire pairing interaction mediated by a SC. This coupling is also known as crossed-Andreev reflection or CPS.^{14,18,19} In the last few years, several CPS experiments have been performed using different platforms, mainly *single* NWs,²⁰⁻²⁴ Carbon Nanotubes^{25,26} and graphene.^{27,28} Splitting efficiencies close to 100% have been reported,²⁶ demonstrating that intrawire pairing can exceed local Cooper pair tunneling. Up to now, all NW based CPS devices consisted of a single NW contacted by two normal metal electrodes and one superconducting contact in between. In order to assess the interwire pairing in double NW structures, it is essential to investigate CPS in such a system. In this work we demonstrate CPS in a parallel double NW device, which is

an important first step towards topological quantum computation with PFs.

II. SCHEME AND SAMPLE

We investigate a device shown schematically in figure 1(a). Two InAs semiconducting NWs with large spin orbit interaction are placed in parallel (NW₁ green, NW₂ red) and electrically coupled by a common superconducting electrode S (blue). Both NWs are contacted by individual normal metal leads N_{1/2} (yellow). Sidegates SG_{1/2} (yellow) are located on each side of the NWs, in order to separately tune the chemical potentials of the quantum dots (QDs), which form between N_{1/2} and S. We note, that the exact location of the QDs is not known, since we do not use additional barrier gates to terminate the QDs.²⁹ However, it is clear that both N_{1/2} and S induce a potential step from which (partial) electron reflection is possible and QD bound states can form. We also point out already here that the electronic boundary conditions on the S side may change if S is in the normal or superconducting state, due to the proximity effect. Besides local Cooper pair tunneling from S to N_{1/2},³⁰ Cooper pairs (white circle with red/black dot) can be split, resulting in a non-local current consisting of entangled single electrons. This process is expected to be large if both QDs, QD_{1/2}, are in resonance and the electrons can sequentially tunnel from the SC to the two normal metal leads.

A. Fabrication and Characterization

The InAs NWs used in this study are grown by Chemical Beam Epitaxy along the $\langle 111 \rangle$ direction. They have a diameter of about 80 nm and possess pure Wurtzite crystal structure. After transferring NWs from the growth chip to the substrate by standard dry transfer, we use scanning electron microscopy, to select NWs naturally lying next to each other. It is important to note that the NWs are electronically disconnected by their native oxide, which is about 2 nm to 3 nm thick surrounding each NW. Next, we deposit the common superconducting lead S made of Ti/Al (thickness: 3 nm/90 nm) after removing the native oxide at the contact area using a solution of $(NH_4)_2S_x$.³¹ Afterwards, the individual normal metal contacts N_{1/2} made of Ti/Au (3 nm/130 nm) are deposited at the same time as the local sidegates SG_{1/2}. A false color scanning electron microscopy image of the device is

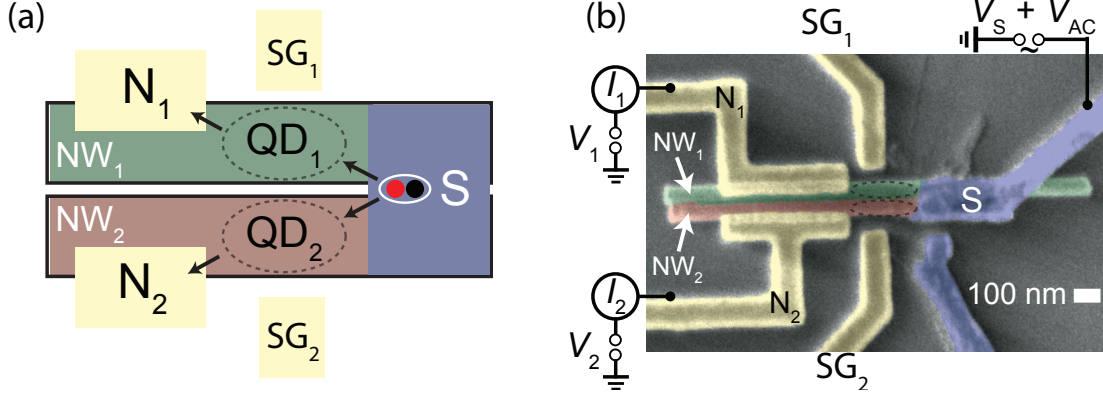


FIG. 1. (a) Schematic depiction of Cooper pair splitting in a double NW setup. Two InAs NWs, $NW_{1/2}$, are located in parallel, coupled by a common superconducting lead S and individual normal metal leads, $N_{1/2}$. $QD_{1/2}$ are tuned separately by local sidegates $SG_{1/2}$. (b) Scanning electron microscope image with false color of the device consisting of $NW_{1/2}$ with a common Al contact (S) on the right and individual Au contacts ($N_{1/2}$) on the left and sidegates, $SG_{1/2}$. The measurement setup is also shown.

shown in figure 1(b). The distance between the source Al contact and the Au drain contacts is about 250 nm.

All measurements were carried out in a dilution refrigerator with a base temperature of about 50 mK. Differential conductance has been measured for the respective NWs simultaneously using synchronized lock-in techniques (see figure 1(b)). Characterization measurements (see figure A1 in appendix) indicate two individual QDs QD_1 and QD_2 in each of the NWs, similar to previous measurements.³² From Coulomb blockade measurements we extract the following parameters for the two QDs for the charging energy U , single particle level spacing ϵ and the life-time broadening of the QD eigenstates Γ to the leads: $U_{1,2} = 0.5 - 0.7$ meV, $\epsilon_1 = 0.3 - 0.5$ meV, $\epsilon_2 = 0.1 - 0.3$ meV, $\Gamma_1 = 0.1 - 0.2$ meV and $\Gamma_2 = 0.2 - 0.3$ meV for QD_1 and QD_2 , respectively. Both quantum dots hold similar properties, implying that each QD is formed between the Al contact and individual Au contacts. In addition, we observe a slight suppression of conductance for some regions within the superconducting energy gap δ of about 150 μ eV, which is similar to other experiments, see appendix.²² We note here, that since $\Delta < \Gamma$, local pair tunneling should exceed CPS.^{26?} We also emphasize that

we cannot distinguish the individual tunnel coupling strengths of each QD to either S or N. The respective tunnel-rate ratio has an important effect on the magnitude of CPS. In particular, CPS can appear to be suppressed in the experiment if tunneling out of the QD into the drain electrode is the rate-limiting step.^{24,26}

III. COOPER PAIR SPLITTING IN DOUBLE NW

In figure 2(a) and 2(b) the simultaneously measured differential conductance G_1 through QD₁ and G_2 through QD₂ are shown, both as a function of the side-gate voltages V_{SG1} and V_{SG2} . These measurement are done at zero bias and without an external magnetic field. Varying the sidegate voltage V_{SG1} tunes QD₁ through several Coulomb blockade resonances, resulting in conductance peaks in G_1 . Similarly V_{SG2} tunes the resonances of QD₂ in NW₂.

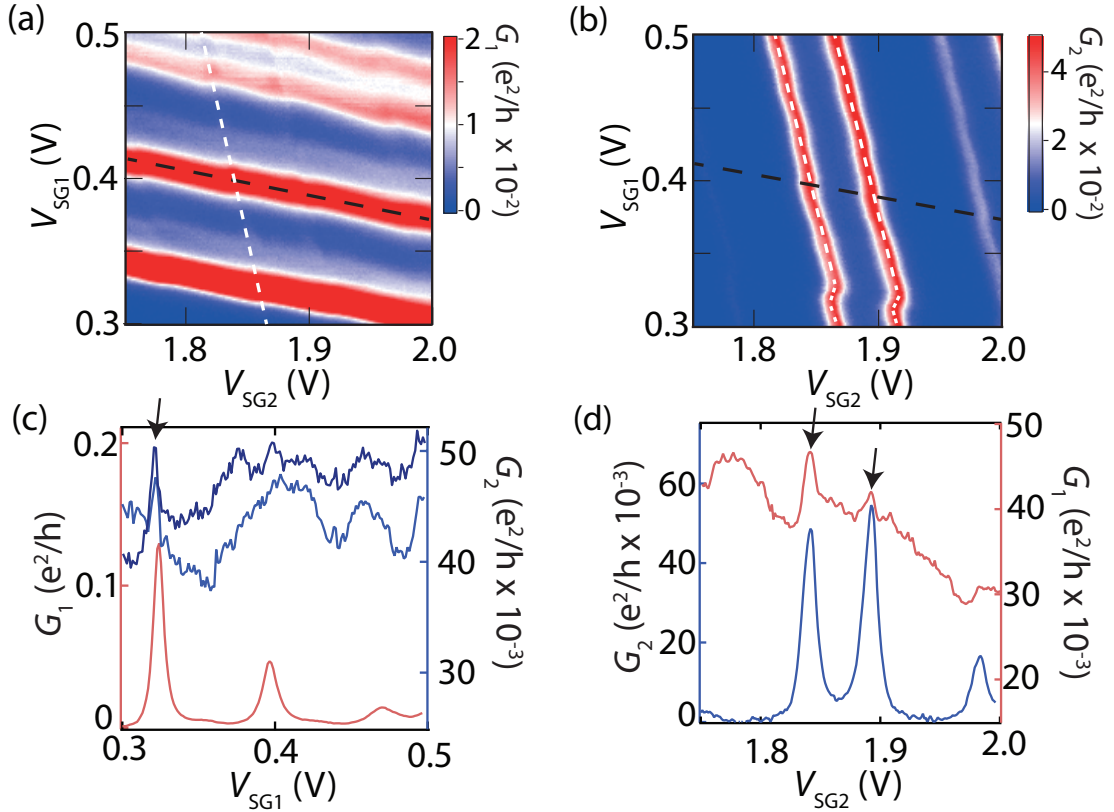


FIG. 2. (a) Differential conductance G_1 of QD₁ as a function of V_{SG1} and V_{SG2} and (b) G_2 respectively for QD₂. (c) cross sections along dashed white lines of (a) and (b). (d) cross section along black dashed line of (a) and (b).

Each resonance signifies a change in charge state of the respective QD. The charge on one QD can be sensed by the other QD, due to the capacitive coupling between QD₁ and QD₂. In our experiment, QD₂ acts as a good sensor for the charge on QD₁, as the Coulomb blockade resonance lines of QD₁ shift whenever the charge on QD₂ changes by one electron, see Fig.2(b). Due to capacitive crosstalk from V_{SG1} on QD₂ (V_{SG2} on QD₁ respectively) the resonance positions are slightly tilted in both graphs. At certain gate voltages, when both QDs are in resonance, an increase of conductance can be observed on both sides. This can be seen more clearly in the cross sections indicated by black and white dashed lines Fig.2(a,b). We observe an enhancement of G_1 along the black dashed line in Fig.2(a) at the peak positions of G_2 for the two resonances at $V_{SG2} \approx 1.87$ V and $V_{SG2} \approx 1.91$ V (see arrows), while other possible correlations are less clear and disappear in the background noise. A similar characteristics can be found in cross sections of G_2 along the white dashed line in Fig.2(b) at peak positions of G_1 . Here, the positive correlation is very clear at $V_{SG1} \approx 0.32$ V (arrow), while there is only a weak quite broadened correlation visible for the other two resonances at $V_{SG1} \approx 0.4$ V and $V_{SG1} \approx 0.49$ V. Hence, we observe clear positive correlation between G_1 and G_2 on three resonances, which we assign to CPS from S into QD₁ and QD₂. We repeat the same measurement in the absence of superconductivity by applying an out of plane magnetic field of 250 mT, which is larger than the critical field of the Al contact. In this case the previously positive correlations between G_1 and G_2 disappear fully, proofing that the positive correlation in conductance originates from CPS (see figure A2 in appendix). We define the CPS efficiency as $2G_{CPS}/G_{total}$ resulting in a maximum efficiency of $\approx 20\%$, similar to the largest reported values on single NW devices.

In the following we investigate the same type of measurement as discussed in figure 2, for a different gate voltage region. The data is shown in figure 3. Here, we observe two sets of resonances for QD₁. Besides the QD levels, we already discussed in figure 2 (indicated with I), we detect a second set of resonances (referred to II). For QD₂ we observe only one set of QD resonances. The resonances denoted with II are significantly different from the one denoted with I. First, the amplitude of type II resonances is only half of the value of type I. Furthermore, type II have a different slope than type I, indicating different capacitive coupling ratio between SG₁ and SG₂. The broadening differs roughly by a factor of two: $\Gamma_I = 0.5$ meV whereas $\Gamma_{II} = 1.2$ meV. Most strikingly, the resonances of type II vanish completely when an external magnetic field is applied, i.e. these resonances are only present in the

superconducting state (not shown). In addition, QD_2 only reacts on a change in charge state of QD_1 for resonances of type I (e.g. green arrow in 3(b)). For the resonances of type II, there seems to be no change in the charge state, as QD_2 does not sense these resonances (e.g. yellow arrows in 3(b)). We therefore conclude that the resonance lines of type II are not Coulomb blockade resonances. They must have their origin within the superconducting phase, most likely near S. Though these features are not Coulomb blockade resonances, they can still be used to test CPS by conductance correlations. We observe a clear positive correlation between the conductances G_1 and G_2 in figure 3(d) as well as in 3(c) for both types of resonances. We estimate a splitting efficiency of about $\approx 13\%$ for type II, which is of similar magnitude as the one obtained for resonances of type II in the gate region of Fig.2.

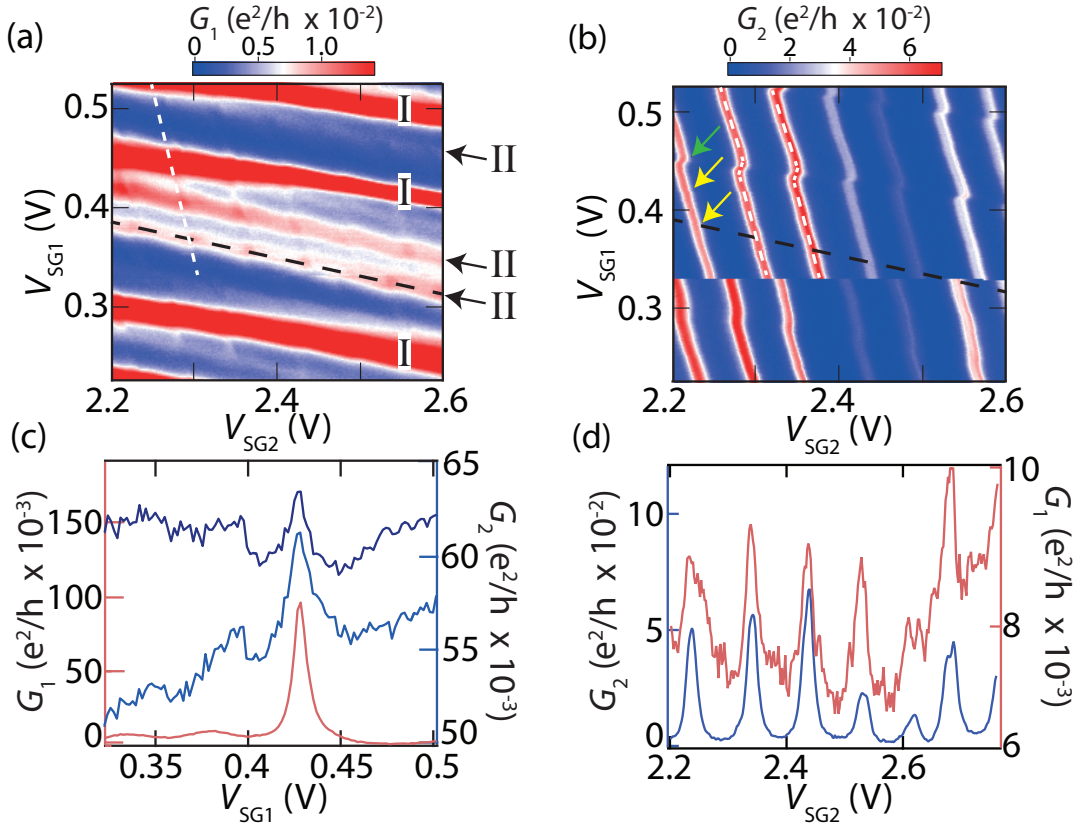


FIG. 3. (a) Differential conductance G_1 of QD_1 as a function of V_{SG1} and V_{SG2} , second set of resonances are denoted with II (black arrows). (b) Differential Conductance G_2 respectively for QD_2 . (c) cross sections along dashed white lines of (a) and (b). (d) cross section along black dashed line of (a) and (b).

The measurements of type II resonances suggest the existence of sub-gap states which are not located in QD_1 , but rather in the lead connecting to S. Since these states are gate-tunable, they are not fully screened by S. We therefore propose that a proximitized region is formed in NW1 that extends to some distance out from S. QD_1 is coupled to this proximitized lead. Within the lead, bound states can form due to potential fluctuations and residual disorder. There are two kinds of bound states, Andreev bound states (ABS)³³⁻³⁵ or Yu-Shiba Rusinov (YSR)³⁶ states. These states do not usually occur at zero energy, but can be tuned electrically to zero energy, signaling a ground state transition between the proximitized lead region and the bulk of the SC. This gives in effect rise to a density-of-state peak in the gap of the SC, enhancing the subgap conductance which we measure. In this case the two electrons that are launched by CPS are transmitted in a different way to the respective drain electrodes. The electron that takes the path through QD_2 is transferred by the usual (resonant) sequential tunneling, while the one that takes the path through QD_1 is transferred by co-tunneling. One might expect that this suppresses CPS as the latter process corresponds to a low probability for out-tunneling into the drain contact. However, due to the sub-gap resonance in the proximitized lead, this process is enhanced and one can therefore reach almost similar CPS efficiencies.

IV. CONCLUSION

In summary, we demonstrate the fabrication of an electronic device, consisting of two closely placed parallel InAs NWs, contacted by a common superconducting lead and individual normal metal leads. By addressing individual sidegates we can separately tune the QDs formed in each NW. When both QDs are in resonance, we observe CPS with efficiencies up to 20%. For certain gate voltages, we detect a second set of QD resonances in one of the NWs, which only appears in the superconducting state. The second set of resonances do not correspond to Coulomb blockade resonances, hence, are not related to a change in the charge state of the QD. Since they only appear in the superconducting state, we tentatively assign the second set to subgap states in the lead that connects to the SC, which are most likely caused by superconducting bound states (Andreev and or Yu-Shiba Rusinov states). For the first time we provide a platform, suitable to implement the next milestone in topological quantum computation, namely Parafermions.

V. ACKNOWLEDGEMENTS

This work was partially supported by a Grant-in-Aid for Young Scientific Research (A) (Grant No. JP15H05407), Grant-in-Aid for Scientific Research (A) (Grant No. JP16H02204), Grant-in-Aid for Scientific Research (S) (Grant No. JP26220710), JSPS Research Fellowship for Young Scientists (Grant No. JP14J10600), and the JSPS Program for Leading Graduate Schools (MERIT) from JSPS, Grants-in-Aid for Scientific Research on Innovative Area Nano Spin Conversion Science (Grants No. JP15H01012 and No. JP17H05177) and a Grant-in-Aid for Scientific Research on Innovative Area Topological Materials Science (Grant No. JP16H00984) from MEXT, JST CREST (Grant No. JPMJCR15N2), Murata Science Foundation and the ImPACT Program of Council for Science, Technology and Innovation (Cabinet Office, Government of Japan). Part of this research was performed within the Nanometer Structure Consortium/NanoLund-environment, using the facilities of Lund Nano Lab, with support from the Swedish Research Council (VR), the Swedish Foundation for Strategic Research (SSF) and from Knut and Alice Wallenberg Foundation (KAW). It was also supported by the Swiss National Science Foundation, the Swiss Nanoscience Institute (SNI), the NCCR on Quantum Science and Technology and the H2020 project QuantERA.

APPENDIX

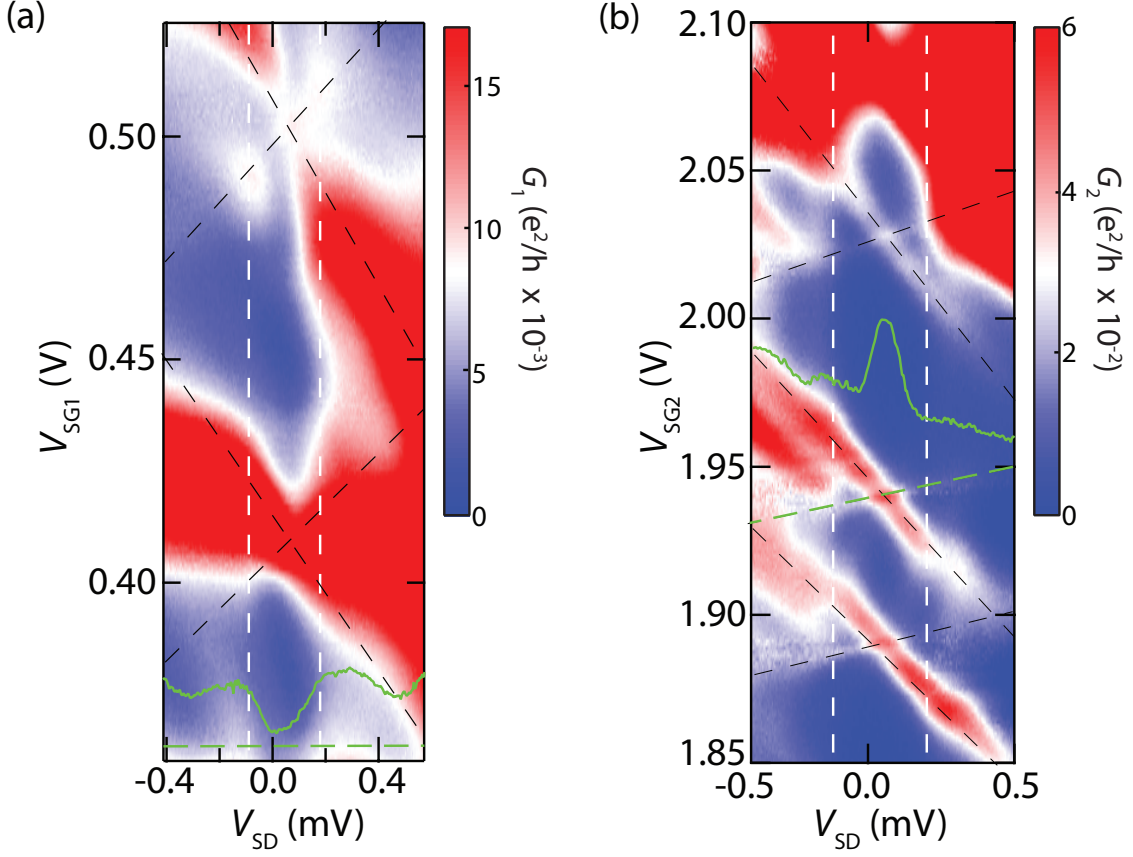


FIG. A1. (a) Differential conductance G_1 of QD_1 as a function of SG_1 and source drain bias V_{SD} . White dashed lines indicate a suppression of conductance due to the superconducting energy gap. Cross section along green dashed line shown in green. (b) Differential conductance G_2 of QD_2 as a function of SG_2 and V_{SD} respectively. Cross section along green dashed line shown in green, representing an enhancement of Andreev Reflection due to the stronger coupling of QD_2 to the SC.

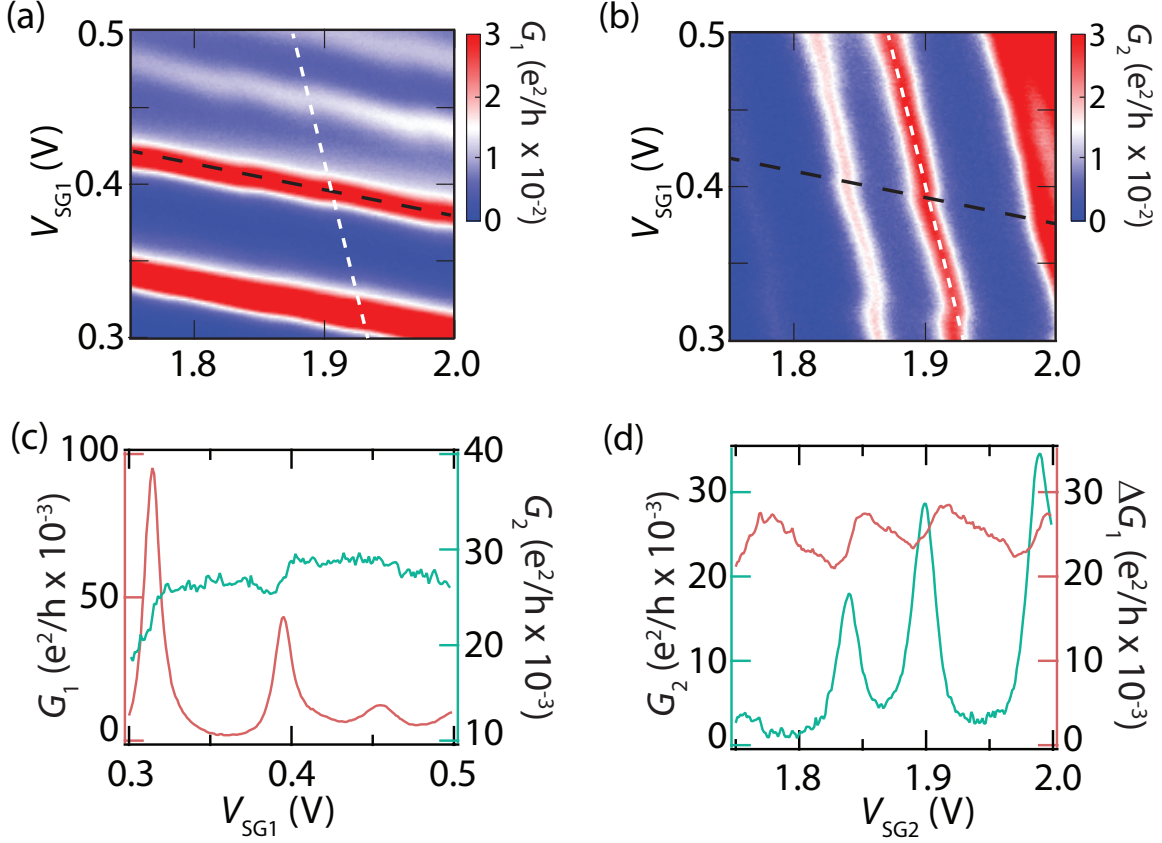


FIG. A2. (a,b) Differential conductance G_1 and G_2 of QD₁ and QD₂ as a function of V_{SG1} and V_{SG2} . During this measurements a constant out-of-plane external magnetic field of 250 mT was applied. (c,d) Cross sections along the dashed white and black lines shown in (a) and (b). The positive correlation, which was evident in Fig. 2 in the main text, is now either absent or replaced by a negative correlation. The latter is expected for classical correlations that can be described by a simple resistor network.²⁰ In (d) a linear background was removed from G_1 , therefore its denoted as ΔG_1 .

REFERENCES

- ¹S. D. Sarma, M. Freedman, and C. Nayak, “Majorana zero modes and topological quantum computation,” *npj Quantum Information* **1**, 15001 (2015).
- ²S. Hoffman, C. Schrade, J. Klinovaja, and D. Loss, “Universal quantum computation with hybrid spin-majorana qubits,” *Physical Review B* **94**, 045316 (2016).

- ³V. Mourik, K. Zuo, S. M. Frolov, S. R. Plissard, E. P. A. M. Bakkers, and L. P. Kouwenhoven, “Signatures of majorana fermions in hybrid superconductor-semiconductor nanowire devices,” *Science* **336**, 1003–1007 (2012).
- ⁴M. T. Deng, C. L. Yu, G. Y. Huang, M. Larsson, P. Caroff, and H. Q. Xu, “Anomalous zero-bias conductance peak in a nb–InSb nanowire–nb hybrid device,” *Nano Letters* **12**, 6414–6419 (2012).
- ⁵S. M. Albrecht, A. P. Higginbotham, M. Madsen, F. Kuemmeth, T. S. Jespersen, J. Nygård, P. Krogstrup, and C. M. Marcus, “Exponential protection of zero modes in majorana islands,” *Nature* **531**, 206–209 (2016).
- ⁶M. T. Deng, S. Vaitiekėnas, E. B. Hansen, J. Danon, M. Leijnse, K. Flensberg, J. Nygård, P. Krogstrup, and C. M. Marcus, “Majorana bound state in a coupled quantum-dot hybrid-nanowire system,” *Science* **354**, 1557–1562 (2016).
- ⁷Ö. Gül, H. Zhang, J. D. S. Bommer, M. W. A. de Moor, D. Car, S. R. Plissard, E. P. A. M. Bakkers, A. Geresdi, K. Watanabe, T. Taniguchi, and L. P. Kouwenhoven, “Ballistic majorana nanowire devices,” *Nature Nanotechnology* (2018), 10.1038/s41565-017-0032-8.
- ⁸J. Alicea, “Majorana fermions in a tunable semiconductor device,” *Physical Review B* **81**, 125318 (2010).
- ⁹Y. Oreg, G. Refael, and F. von Oppen, “Helical liquids and majorana bound states in quantum wires,” *Physical Review Letters* **105**, 177002 (2010).
- ¹⁰J. K. Pachos, *Introduction to Topological Quantum Computation* (Cambridge University Press, 2012).
- ¹¹A. Keselman, L. Fu, A. Stern, and E. Berg, “Inducing time-reversal-invariant topological superconductivity and fermion parity pumping in quantum wires,” *Physical Review Letters* **111**, 116402 (2013).
- ¹²J. Klinovaja and D. Loss, “Time-reversal invariant parafermions in interacting rashba nanowires,” *Physical Review B* **90**, 045118 (2014).
- ¹³E. Gaidamauskas, J. Paaske, and K. Flensberg, “Majorana bound states in two-channel time-reversal-symmetric nanowire systems,” *Physical Review Letters* **112**, 233513 (2014).
- ¹⁴K. Sato, D. Loss, and Y. Tserkovnyak, “Crossed andreev reflection in quantum wires with strong spin-orbit interaction,” *Physical Review B* **85**, 235433 (2012).
- ¹⁵C. Bena, S. Vishveshwara, L. Balents, and M. P. A. Fisher, “Quantum entanglement in carbon nanotubes,” *Physical Review Letters* **89**, 037901 (2002).

- ¹⁶P. Recher and D. Loss, “Superconductor coupled to two luttinger liquids as an entangler for electron spins,” *Physical Review B* **65**, 165327 (2002).
- ¹⁷M. Thakurathi, P. Simon, I. Mandal, J. Klinovaja, and D. Loss, “Majorana kramers pairs in rashba double nanowires with interactions and disorder,” *Physical Review B* **97**, 045415 (2018).
- ¹⁸P. Recher, E. V. Sukhorukov, and D. Loss, “Andreev tunneling, coulomb blockade, and resonant transport of nonlocal spin-entangled electrons,” *Physical Review B* **63**, 165314 (2001).
- ¹⁹D. Chevallier, J. Rech, T. Jonckheere, and T. Martin, “Current and noise correlations in a double-dot cooper-pair beam splitter,” *Phys. Rev. B* **83**, 125421 (2011).
- ²⁰L. Hofstetter, S. Csonka, J. Nygård, and C. Schönenberger, “Cooper pair splitter realized in a two-quantum-dot y-junction,” *Nature* **461**, 960–963 (2009).
- ²¹L. Hofstetter, S. Csonka, A. Baumgartner, G. Flp, S. d’Hollosy, J. Nygård, and C. Schönenberger, “Finite-bias cooper pair splitting,” *Physical Review Letters* **107**, 136801 (2011).
- ²²A. Das, Y. Ronen, M. Heiblum, D. Mahalu, A. V. Kretinin, and H. Shtrikman, “High-efficiency cooper pair splitting demonstrated by two-particle conductance resonance and positive noise cross-correlation,” *Nature Communications* **3**, 2169 (2012).
- ²³G. Fülöp, S. d’Hollosy, A. Baumgartner, P. Makk, V. A. Guzenko, M. H. Madsen, J. Nygård, C. Schönenberger, and S. Csonka, “Local electrical tuning of the nonlocal signals in a cooper pair splitter,” *Physical Review B* **90**, 235412 (2014).
- ²⁴G. Fülöp, F. Domínguez, S. d’Hollosy, A. Baumgartner, P. Makk, M. Madsen, V. Guzenko, J. Nygård, C. Schönenberger, A. L. Yeyati, and S. Csonka, “Magnetic field tuning and quantum interference in a cooper pair splitter,” *Physical Review Letters* **115**, 227003 (2015).
- ²⁵L. G. Herrmann, F. Portier, P. Roche, A. L. Yeyati, T. Kontos, and C. Strunk, “Carbon nanotubes as cooper-pair beam splitters,” *Physical Review Letters* **104**, 026801 (2010).
- ²⁶J. Schindele, A. Baumgartner, and C. Schönenberger, “Near-unity cooper pair splitting efficiency,” *Physical Review Letters* **109**, 157002 (2012).
- ²⁷Z. Tan, D. Cox, T. Nieminen, P. Lhteenmki, D. Golubev, G. Lesovik, and P. Hakonen, “Cooper pair splitting by means of graphene quantum dots,” *Physical Review Letters* **114**, 096602 (2015).

- ²⁸I. V. Borzenets, Y. Shimazaki, G. F. Jones, M. F. Craciun, S. Russo, M. Yamamoto, and S. Tarucha, “High efficiency CVD graphene-lead (pb) cooper pair splitter,” *Scientific Reports* **6**, 23051 (2016).
- ²⁹C. Fasth, A. Fuhrer, M. T. Bjrk, and L. Samuelson, “Tunable double quantum dots in inas nanowires defined by local gate electrodes,” *Nano Letters* **5**, 1487–1490 (2005).
- ³⁰J. Gramich, A. Baumgartner, and C. Schönenberger, “Resonant and inelastic andreev tunneling observed on a carbon nanotube quantum dot,” *Physical Review Letters* **115**, 216801 (2015).
- ³¹D. B. Suyatin, C. Thelander, M. T. Bjrk, I. Maximov, and L. Samuelson, “Sulfur passivation for ohmic contact formation to InAs nanowires,” *Nanotechnology* **18**, 105307 (2007).
- ³²S. Baba, S. Matsuo, H. Kamata, R. S. Deacon, A. Oiwa, K. Li, S. Jeppesen, L. Samuelson, H. Q. Xu, and S. Tarucha, “Gate tunable parallel double quantum dots in InAs double-nanowire devices,” *Applied Physics Letters* **111**, 233513 (2017).
- ³³J.-D. Pillet, C. H. L. Quay, P. Morfin, C. Bena, A. L. Yeyati, and P. Joyez, “Andreev bound states in supercurrent-carrying carbon nanotubes revealed,” *Nature Physics* **6**, 965–969 (2010).
- ³⁴T. Dirks, T. L. Hughes, S. Lal, B. Uchoa, Y.-F. Chen, C. Chialvo, P. M. Goldbart, and N. Mason, “Transport through andreev bound states in a graphene quantum dot,” *Nature Physics* **7**, 386–390 (2011).
- ³⁵J. Gramich, A. Baumgartner, and C. Schönenberger, “Andreev bound states probed in three-terminal quantum dots,” *Physical Review B* **96**, 195418 (2017).
- ³⁶A. Jellinggaard, K. Grove-Rasmussen, M. H. Madsen, and J. Nygård, “Tuning yu-shiba-rusinov states in a quantum dot,” *Physical Review B* **94**, 064520 (2016).